

## Aggregation Behavior of Tetrakis(4-sulfonatophenyl)porphyrin in AOT/Water/Decane Microemulsions

Maria Angela Castriciano,<sup>†</sup> Andrea Romeo,<sup>†</sup> Valentina Villari,<sup>‡</sup> Nicola Angelini,<sup>‡</sup> Norberto Micali,<sup>‡</sup> and Luigi Monsù Scolaro<sup>\*,†</sup>

Dipartimento di Chimica Inorganica, Chimica Analitica e Chimica Fisica, Università di Messina, Salita Sperone 31, 98166 Vill. S. Agata, Messina, Italy, and CNR, Istituto per i Processi Chimico-Fisici, Sez. Messina, Via La Farina 237, 98123 Messina, Italy

Received: February 21, 2005; In Final Form: April 26, 2005

AOT/water/decane microemulsions have been used to entrap the water-soluble 5,10,15,20-tetrakis(4-sulfonatophenyl)porphyrin (TPPS<sub>4</sub>). Quasi-elastic light scattering technique has confirmed the confinement of the porphyrin and its various aggregates into the inner water pool. Various species have been detected as function of the size of the microemulsions, concentration of the porphyrin, pH, and aging of the solutions by using a combination of UV–vis absorption, steady fluorescence emission, fluorescence lifetime measurements, and time-resolved fluorescence anisotropy. Under neutral pH conditions, the porphyrin is present as the free base monomer (S<sub>414</sub>) in the inner water compartment, and it is free to rotate when the size of the droplet is large enough and the porphyrin concentration is low. On increasing the concentration and/or decreasing the microemulsion size, a H-dimer of the free base (S<sub>406</sub>) is prevalently formed. Aging both the S<sub>414</sub> and S<sub>406</sub> species leads to the formation of a new species (S<sub>424</sub>), which has been postulated as a H-type dimer of the diacid porphyrin. On decreasing the pH, the species S<sub>414</sub> and S<sub>406</sub> almost instantaneously convert into the diacid porphyrin, which is monomeric (S<sub>434</sub>). This latter is an intermediate in the eventual formation of J-aggregated TPPS<sub>4</sub> (S<sub>490</sub>). A marked stability has been observed for the S<sub>424</sub> species, which do not interconvert on changing the pH of the bulk aqueous phase.

### Introduction

Aggregation is a well-known phenomenon in porphyrin chemistry, and its occurrence has a deep impact on many physicochemical properties of these molecules.<sup>1</sup> Depending on the geometrical disposition of the chromophores, the exciton theory developed by Kasha predicts the occurrence of hypsochromic or bathochromic shifts for the relevant absorption bands, in the case of H (*face-to-face*) or J-type (*side-by-side*) interactions, respectively.<sup>2,3</sup>

During the past decade, the water-soluble 5,10,15,20-tetrakis(4-sulfonatophenyl)porphyrin (TPPS<sub>4</sub>) has been largely investigated by many authors mainly because its diacid form is able to self-aggregate, leading to ordered nanowires of J-aggregates<sup>4</sup> having interesting photophysical properties<sup>5–9</sup> and potentially suitable for optoelectronic applications.<sup>10</sup> The free base TPPS<sub>4</sub> is a tetra-anion because of the presence of four negatively charged sulfonate groups on the meso aryl substituent groups. The central nitrogen atoms exhibit a  $pK_a \sim 4.9$ ,<sup>11</sup> consequently, at neutral pH values, this molecule is present as the free base, which is monomeric. Dimerization of this form has been evidenced only in the presence of crown ethers and alkali metal ions.<sup>12</sup> At pH values lower than 4, the zwitterionic diacid form is prevalently present in solution. This species is a dianion and, increasing the acidity and the ionic strength of the solutions, aggregation occurs. Under these experimental conditions, both

H- and J-aggregates have been reported.<sup>4,13–29</sup> In particular, the J-aggregate form has been proposed to be stabilized through a network of electrostatic and hydrogen-bonding interactions mainly involving the negatively charged sulfonate groups and the positively charged inner nitrogen core.<sup>15,17</sup> The exciton delocalization over a high number of monomer units and the motional narrowing, which mediates the local inhomogeneities,<sup>30</sup> has been invoked to explain the occurrence of a sharp and consistently red-shifted B-band. In a micellar phase with different kind of surfactants,<sup>31–33</sup> in assembled monolayers<sup>34,35</sup> in mesoporous aluminosilicate,<sup>36</sup> or in the presence of templating polymeric matrixes, e.g., aminoterminated dendrimers<sup>37,38</sup> and charged polymers,<sup>28,39–41</sup> both J- and H-aggregates have been observed.

Recently, we have reported on the confinement of J-aggregates of TPPS<sub>4</sub> in the water pool of AOT (sodium bis(2-ethylhexyl)sulfosuccinate) water in oil microemulsions.<sup>42</sup> This particular system has been selected because its phase diagram is very well-known in the literature.<sup>43–46</sup> Changing the ratio  $w_0 = [\text{water}]/[\text{AOT}]$ , it is very easy to control the dimension of the inner water pool and hence to modulate the interaction between the guest molecule (i.e., the porphyrin) and the internal components of the microemulsion. In particular, the surfactant is anionic, and the charged sulfonate groups are oriented toward the inner water pool, creating an ionic double layer, which exerts an effect on the included molecules in terms of local or effective pH and ionic strength.<sup>47</sup> Many other examples of porphyrin inclusion have already been reported in the literature.<sup>48–51</sup> In the case of TPPS<sub>4</sub>, we succeeded in obtaining nanosized J-aggregates exhibiting spectroscopic coherence values close to unity (i.e., the exciton is delocalized on the entire aggregate),

\* Author to whom correspondence should be addressed. E-mail: monsu@chem.unime.it. Telephone: +39 090 6765711. Fax: +39 090 393756.

<sup>†</sup> Università di Messina.

<sup>‡</sup> Istituto per i Processi Chimico-Fisici.

much higher than those reported for similar systems grown in bulk solution with ammonium salt.<sup>52</sup>

In this paper, we report a spectroscopic and photophysical characterization of all the species present in this confined system under different experimental conditions (pH of the bulk solution, porphyrin concentration, and  $w_0$  values). On varying the microemulsion size and porphyrin concentration or on aging the solutions, we anticipate that new aggregated species, exhibiting the spectroscopic features of H-dimers, have been identified.

## Experimental Section

5,10,15,20-Tetrakis(4-sulfonatophenyl)porphyrin (TPPS<sub>4</sub>) tetrasodium salt was purchased from Aldrich Co. Stock solutions of TPPS<sub>4</sub> (up to 20 mM) were prepared in dust-free Millipore water, stored in the dark, and freshly used. High purity AOT (Fluka, 99%) and decane (Aldrich, spectrophotometric grade) were used as received.

Microemulsions were prepared by mixing AOT, decane, and water in the proper ratio and equilibrated for a week. The ratio  $w_0 = [\text{water}]/[\text{AOT}]$  was changed in the range 6–65 (6, 14, 23, 32, 34, 43, 54, 65), corresponding to measured hydrodynamic radii  $R_H = 25, 40, 55, 68, 75, 90, 110$ , and  $170 \text{ \AA}$ , respectively, through quasi-elastic light scattering (QELS). The volume fraction  $\phi$  was kept at 0.05. The effective hydrodynamic radii were measured before mixing and after reaching equilibrium. In all the cases, we found that the dimensions do not change, and they correspond to those obtained for microemulsions containing only water at each  $w_0$ . This finding points to the fact that the species are effectively confined into the water pool. As pointed out in the Results Section, aggregation occurred only for  $w_0 \geq 32$ , and it was achieved by mixing equal volume of microemulsions containing concentrated porphyrin in water (80  $\mu\text{M}$ ) and citrate buffer at the selected pH and ionic strength.

UV–vis spectra were obtained on a Hewlett-Packard model 8453 diode array spectrophotometer using 1-cm path length quartz cells. The UV–vis spectra were deconvoluted using Gaussian component bands through PeakFit v. 4.0 software package (SPSS Inc.). Fluorescence emission and resonance light scattering (RLS) experiments were performed on a Jasco model FP-750 spectrofluorometer, adopting for RLS experiments a synchronous scan protocol with a right-angle geometry.<sup>53</sup> Fluorescence emission and RLS spectra were not corrected for the absorption of the samples. Fluorescence quantum yields of aerated solutions were determined relative to that of TPPS<sub>4</sub> in water ( $\phi_f \approx 0.12$ )<sup>54</sup> with the appropriate corrections for the refractive index of the solvent.

**Quasielastic Light Scattering.** QELS measurements were carried out using the 532 nm line of a doubled Nd:YAG laser as excitation source and an experimental apparatus already described.<sup>26,42</sup> The temperature was kept fixed within  $\pm 0.01 \text{ K}$ . The QELS measurements were performed at different scattering wavevectors,  $k$  (being  $k = [(4\pi n)/\lambda] \sin(\theta/2)$ , where  $n$  is the refractive index of the sample and  $\lambda$  the wavelength of the incident light in the vacuum). The observed linear behavior of the relaxation rates on  $k^2$  indicates the diffusive nature of the detected relaxations.<sup>55–57</sup> In a QELS experiment, the measured intensity correlation function  $g^{(2)}(t)$  is related to the electric field correlation function,  $g^{(1)}(t)$ , by the Siegert relation:<sup>55–57</sup>

$$g^{(2)}(t) = B(1 + f|g^{(1)}(t)|^2) \quad (1)$$

where  $B$  is the baseline and  $f$  is a spatial coherence factor. In

the case of dilute solutions of monodispersed particles  $g^{(1)}(t) = \exp(-k^2Dt)$ , where  $D$  is the translational diffusion coefficient. From the diffusion coefficient  $D$ , the mean hydrodynamic radius  $R_H$  of diffusing particles can be calculated using the equation:

$$D = \frac{k_B T}{6\pi\eta R_H} \quad (2)$$

where  $k_B$  is the Boltzmann constant,  $T$  is the absolute temperature, and  $\eta$  is the viscosity of the solvent. In general,  $g^{(1)}(t)$  may be expressed as the Laplace transform of a continuous distribution  $G(\Gamma)$  of decay times (relaxation rates  $\Gamma$ ).<sup>55–57</sup> The effective diffusion coefficient  $D(k) = [\Gamma(k)/k^2]$  can be obtained from the standard second-order cumulant analysis of the autocorrelation functions.<sup>58,59</sup>

**Photophysical Measurements.** All fluorescence measurements were carried out by a time-correlated-single-photon-counting (TCSPC)<sup>60</sup> homemade apparatus. As previously described,<sup>61</sup> an argon ion laser, operating in the mode-locked regime (514 nm) at a repetition rate of 82 MHz, is used to synchronously pump a Rhodamine 6G dye laser. In this way, the excitation beam, focused on the sample, is constituted by laser pulses of  $\sim 2 \text{ ps}$  fwhm at 570 nm wavelength, vertically polarized by a Glan–Taylor polarizer. The fluorescence photons (collected at  $90^\circ$ ) passed through a monochromator, modified to avoid any effects due to the different transmission efficiency for vertically and horizontally polarized light, and were detected with a microchannel-plate photomultiplier (Hamamatsu R1645U-01,  $\sim 200 \text{ ps}$  rise time). The time resolution of the detection system was measured by examining scattering light from the excitation pulse, giving for the overall instrumental response a half-width value of about 200 ps at half height. The instrumental resolution (corresponding to the minimum measurable time value) was about few tens of picoseconds after analyzing the fluorescence decay profiles by using the nonlinear least-squares iterative reconvolution procedures on the basis of the Marquardt algorithm.<sup>62</sup> In the case of total fluorescence decay curves, the fitting was performed on the basis of the multiexponential decay law:

$$I(t) = I_0 \sum_i \alpha_i \exp(-t/\tau_i) \quad (3)$$

where  $I(t)$  is total fluorescence decay curve,  $I_0$  is the intensity at time zero, and  $\alpha_i$  and  $\tau_i$  are, respectively, relative amplitude and lifetime of  $i$ th.<sup>63</sup>

Fluorescence anisotropy ( $r(t)$ ) is defined using the following expression:

$$r(t) = \frac{I_{VV}(t) - I_{VH}(t)}{I_{VV}(t) + 2I_{VH}(t)} \quad (4)$$

where VV and VH indicate, respectively, the vertically and horizontally polarized emission, the excitation beam being vertically polarized.<sup>63</sup> Because the anisotropy decay times, in our experimental conditions, were much longer than the overall instrumentation response ( $\sim 200 \text{ ps}$ ), the  $r(t)$  curves were directly fitted, without deconvolution procedure, on the basis of exponential decay law:<sup>63</sup>

$$r(t) = \sum_j r_{0j} \exp(-t/\tau_{Rj}) \quad (5)$$

where  $\sum_j r_{0j}$  is the limiting anisotropy in the absence of rotational diffusion, and  $\tau_{Rj}$  is the individual rotational correlation time.

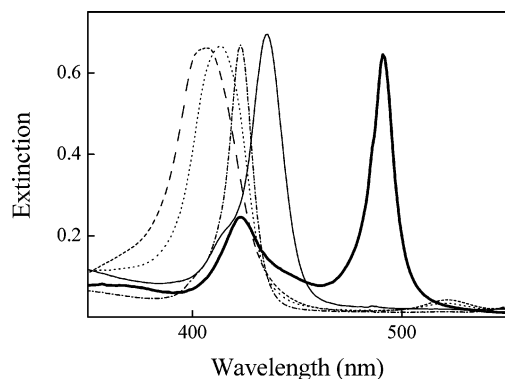


**Figure 1.** UV-vis spectra of the various TPPS<sub>4</sub> species present in AOT microemulsions at 293 K under different experimental conditions: S<sub>406</sub>, ( $w_0 = 32$ , [TPPS<sub>4</sub>] = 5 mM in water, dashed line), S<sub>414</sub>, ( $w_0 = 32$ , [TPPS<sub>4</sub>] = 80  $\mu$ M in water, dotted line), S<sub>424</sub>, ( $w_0 = 32$ , [TPPS<sub>4</sub>] = 80  $\mu$ M in water after 10 days, dashed-dotted line), S<sub>434</sub>, ( $w_0 = 32$ , [TPPS<sub>4</sub>] = 80  $\mu$ M, pH 2.7 citrate buffer 50 mM, solid line), S<sub>490</sub>, ( $w_0 = 32$ , [TPPS<sub>4</sub>] = 80  $\mu$ M, pH 2.7 citrate buffer 50 mM after 2 h, marked line).

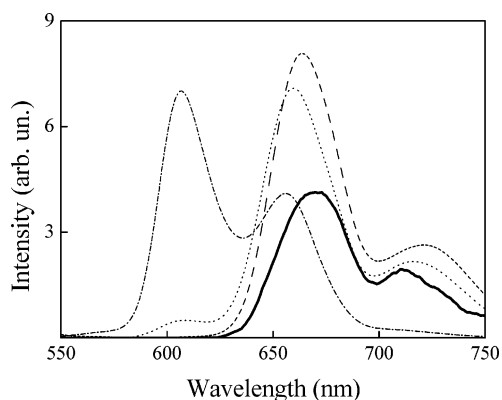


**Figure 2.** Fluorescence emission spectra of the various TPPS<sub>4</sub> species present in AOT microemulsions at 293 K under different experimental conditions: S<sub>406</sub>, ( $w_0 = 32$ , [TPPS<sub>4</sub>] = 5 mM in water, dashed line), S<sub>414</sub>, ( $w_0 = 32$ , [TPPS<sub>4</sub>] = 80  $\mu$ M in water, dotted line), S<sub>424</sub>, ( $w_0 = 32$ , [TPPS<sub>4</sub>] = 80  $\mu$ M in water after 10 days, dashed-dotted line), S<sub>490</sub>, ( $w_0 = 32$ , [TPPS<sub>4</sub>] = 80  $\mu$ M, pH 2.7 citrate buffer 50 mM after 2 h, marked line),  $\lambda_{\text{ex}} = 520$  nm.

In the simple case of “spherical molecules”,  $\tau_{Rj}$  is related to the volume ( $V_j$ ) of the equivalent sphere by the following equation:

$$\tau_{Rj} = \frac{\eta V_j}{k_B T} \quad (6)$$

where  $\eta$  is the microviscosity of the medium,  $T$  is the absolute temperature, and  $k_B$  is the Boltzmann constant.

## Results

Different spectroscopic evidence points out the occurrence of various species in the water pool of the microemulsions as function of the  $w_0$  ratio, the concentration of porphyrin, and the pH of the bulk solutions. In the following text, we will indicate these species, referring to the corresponding position of the Soret band (e.g., S<sub>406</sub> for the species exhibiting a B-band at 406 nm). Typical UV-vis absorption and fluorescence emission spectra for the various species, obtained under different experimental conditions, are reported in Figures 1 and 2, while all their relevant spectroscopic data are collected in Table 1.

**Effect of the Microemulsion Size.** The impact of the water pool size has been investigated by fixing the concentration of TPPS<sub>4</sub> at 80  $\mu$ M in water and changing the  $w_0$  value in the

**TABLE 1: UV-vis Absorption and Fluorescence Emission Maxima with Relative Quantum Yields for the Various TPPS<sub>4</sub> Species in AOT/Water/Decane Microemulsions at 293 K**

	B-band (nm)	Q-bands (nm)	$\lambda_{\text{em}}$ (nm)	$\phi_r$
S <sub>406</sub>	406	522, 560, 592, 651	660, 724	0.07
S <sub>414</sub>	414	520, 560, 596, 648	657, 712	0.09
S <sub>424</sub>	424	558, 600	606, 656	0.006
S <sub>434</sub>	434	595, 647		
S <sub>490</sub>	490	635, 706	670, 714	

range 6–65 ( $\phi = 0.05$ ). As expected, on increasing the  $w_0$  value, the extinction of the various samples increases because of the increasing amount of TPPS<sub>4</sub> in the droplets. At  $w_0 < 23$ , the UV-vis absorption spectra show two intense B-bands located at 406 and 414 nm, accompanied by a series of at least four weaker Q-bands (Figure 3). The corresponding emission spectra exhibit two bands at 660 and 724 nm (inset Figure 3). At  $w_0 \geq 23$ , the UV-vis spectra change to a well-defined species having a B-band located at 414 nm and four Q-bands at 520, 560, 596, and 648 nm. The emission spectra gradually change, evidencing three new peaks at 606, 657, and 712 nm.

On standing, the systems with  $w_0 \geq 23$  show characteristic spectral changes. The UV-vis spectra display the gradual disappearance of the B-band at 414 nm with the formation of a new band at 424 nm, together with two Q-bands at 558 and 600 nm. After 10 days, S<sub>424</sub> is the only component in the microemulsions. The final emission spectra show two blue-shifted bands at 606 and 656 nm (inset of Figure 4).

Over the investigated  $w_0$  range, RLS spectra of the various samples evidenced profiles corresponding to normal Rayleigh

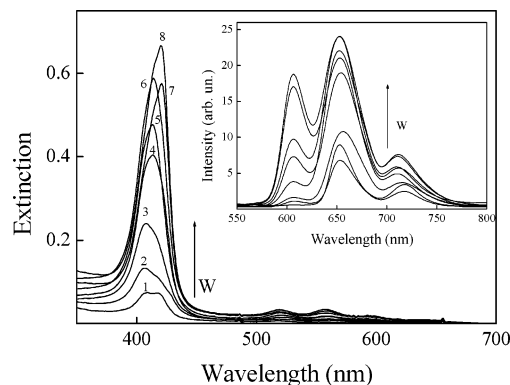


**Figure 3.** UV-vis spectra of freshly prepared samples of TPPS<sub>4</sub> in AOT/water/decane microemulsions ([TPPS<sub>4</sub>] = 80  $\mu$ M,  $\phi = 0.05$ ,  $T = 293$  K) at different increasing  $w_0$  values (6–65). Inset: corresponding fluorescence emission ( $\lambda_{\text{ex}} = 420$  nm) spectra.

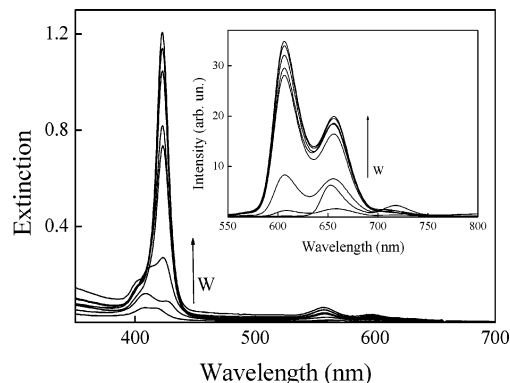


**Figure 4.** UV-vis spectra of aged samples (10 days) of TPPS<sub>4</sub> in AOT/water/decane microemulsions ([TPPS<sub>4</sub>] = 80  $\mu$ M,  $\phi = 0.05$ ,  $T = 293$  K) at different increasing  $w_0$  values (6–65). Inset: corresponding fluorescence emission ( $\lambda_{\text{ex}} = 420$  nm) spectra.



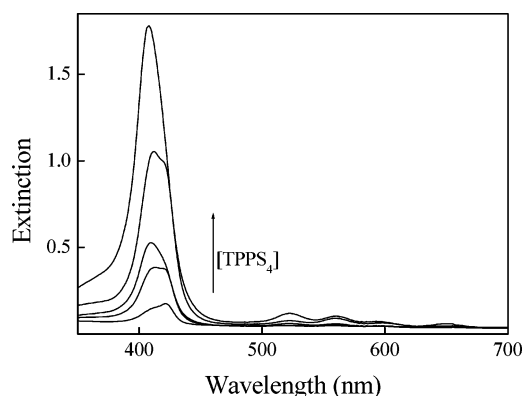


**Figure 5.** UV-vis spectra of samples of TPPS<sub>4</sub> in AOT/water/decane microemulsions ( $w_0 = 32$ ,  $\phi = 0.05$ ,  $T = 293$  K) at different increasing porphyrin concentration (0.2, 0.5, 1, 3 and 5 mM).

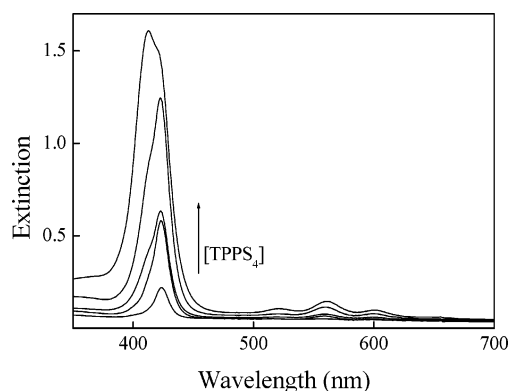


**Figure 6.** UV-vis spectra of aged (3 days) samples of TPPS<sub>4</sub> in AOT/water/decane microemulsions ( $w_0 = 32$ ,  $\phi = 0.05$ ,  $T = 293$  K) at different increasing porphyrin concentration (0.2, 0.5, 1, 3, and 5 mM).

scattering because of the microemulsions, as well as diminished scattering intensities at frequencies corresponding to the absorption bands (data not shown).

As already reported,<sup>42</sup> on decreasing pH by mixing equal volumes of aqueous TPPS<sub>4</sub> and citrate buffer (pH = 2.7, 50 mM) in microemulsions, only for  $w_0 \geq 32$ , the UV-vis spectra clearly display the almost instantaneous formation of a species with a Soret band at 434 nm and two less intense Q-bands at 595 and 647 nm (solid line in Figure 1). This species eventually converts into a final species characterized by a narrow and red-shifted peak at 490 nm, a broader and less intense one at 423 nm, and three Q-bands at 637, 671, and 709 nm (marked line in Figure 1).

**Effect of the Porphyrin Concentration.** This effect has been studied by fixing the microemulsion size ( $w_0 = 32$ ,  $\phi = 0.05$ ) and changing the TPPS<sub>4</sub> concentration in the range of 0.2–5 mM. The UV-vis spectra show the presence of two species having the most prominent absorption features at 406 and 414 nm (Figure 5). On increasing the porphyrin concentration, S<sub>406</sub> becomes the dominant species in solution. The emission spectra evidence the occurrence of three main peaks at 606, 658, and 724 nm, which gradually evolve into a final spectrum with features at 606 and 656 nm (data not shown).

The aging of all these samples causes spectral changes affording the S<sub>424</sub> species, as already described in the previous section (Figure 6).

To gain information on the S<sub>406</sub> and S<sub>414</sub> species, further experiments have been performed. Reverse micelles have been prepared, starting with anhydrous decane and AOT, and TPPS<sub>4</sub> has been included in such systems. The UV-vis spectra of such

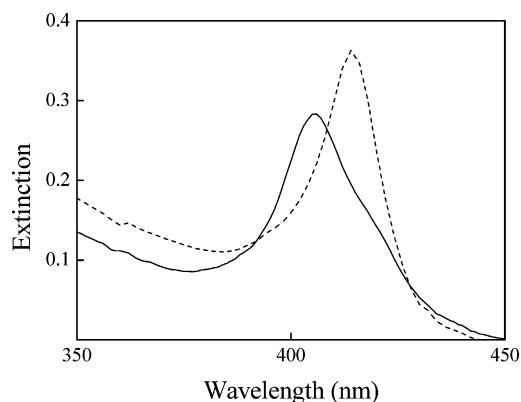


**Figure 7.** UV-vis spectra of TPPS<sub>4</sub> in microemulsions: solid line, in inverted micelles ( $w_0$  virtually 0); dashed line,  $w_0 = 32$ , [TPPS<sub>4</sub>] = 5  $\mu$ M, 8-cm path length.

samples evidence a B-band centered at 406 nm and an additional minor band at 414 nm (Figure 7, solid line). The corresponding fluorescence emission spectra display two major components at 660 and 724 nm. On the other hand, starting from a diluted porphyrin stock solution ([TPPS<sub>4</sub>] = 5  $\mu$ M), we have obtained a sample in which S<sub>414</sub> is the predominant species (Figure 7, dashed line).

**Stability of S<sub>424</sub> and S<sub>406</sub> Species.** The species S<sub>424</sub>, obtained on aging the TPPS<sub>4</sub>/microemulsion systems ( $w_0 \geq 23$ ) under neutral pH conditions, is quite stable to further pH changes. Indeed, the UV-vis and fluorescence spectra do not change appreciably on mixing equal volumes of preformed S<sub>424</sub> ([TPPS<sub>4</sub>] = 5 mM,  $w_0 = 32$ ,  $\phi = 0.05$ ) either with NaOH 0.01 M or with citrate buffer at pH 2.7 (50 mM) in AOT/water/decane microemulsions.

Analogously, the species S<sub>406</sub> ([TPPS<sub>4</sub>] = 3 mM,  $w_0 = 32$ ,  $\phi = 0.05$ ) remains unaltered on treatment with NaOH 0.01 M in AOT/water/decane microemulsions.

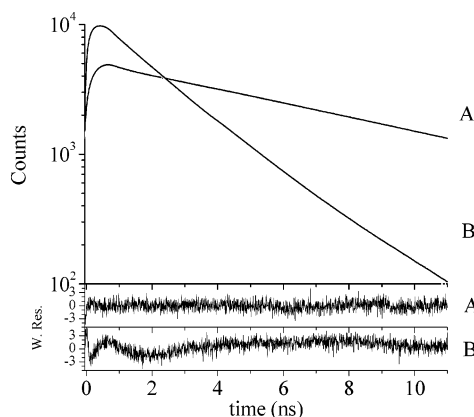
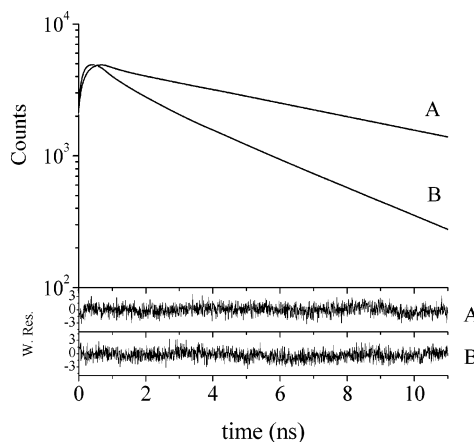
**Fluorescence Lifetimes and Time-Resolved Anisotropy Investigations.** Time-resolved fluorescence measurements were performed at 293 K on different samples, mainly containing S<sub>414</sub>, S<sub>490</sub>, S<sub>406</sub> (emission detected at 660 nm), and S<sub>424</sub> (emission detected at 606 nm). All lifetime values with their relative amplitudes are reported in the first six columns of Table 2, whereas, Figures 8 and 9 show the fluorescence decay curves and the relative fitting curves for S<sub>424</sub>, S<sub>406</sub> and S<sub>414</sub>, S<sub>490</sub>, respectively, together with a typical weighted residuals plot to evaluate the goodness of the fit. In the case of S<sub>414</sub> and S<sub>406</sub>, the emission decays of TPPS<sub>4</sub> show a biexponential behavior with a long lifetime value of about 8 ns, which is prevalent (its relative amplitude being 59% for S<sub>414</sub> and 52% for S<sub>406</sub>), and a shorter one of about 0.5 ns. Completely different is the emission of S<sub>490</sub> and S<sub>424</sub>, whose decays are well fitted with triexponential curves (see Table 2). In these latter samples, the prevalent emitting species is a very short-living component with a lifetime value of 0.11 ns for S<sub>490</sub> (relative amplitude of 96%) and 0.07 ns for S<sub>424</sub> (relative amplitude of 99%), respectively.

Fluorescence anisotropy decays ( $r(t)$ ) for TPPS<sub>4</sub> in the samples (together with the fitting curves) are shown in Figure 10, and the related parameters ( $r_{0j}$  and  $\tau_{Rj}$ ), calculated by fitting the anisotropy curves, are reported in the last four columns of Table 2. In the case of S<sub>414</sub>, the fluorescence emission is completely depolarized, and the  $r(t)$  curve appears as a “stochastic” oscillation around the zero value. This fact can probably be due to the relative angle between the absorption and emission dipoles, which, in our conditions, could be close to the magic angle (54.7°), leading to an anisotropy value ( $r_0$ ) equal to zero.

**TABLE 2: Fluorescence Photophysical Parameters (Lifetimes, Relative Amplitude, Initial Anisotropy, and Rotational Correlation Times) for the Various TPPS<sub>4</sub> Species in AOT/Water/Decane Microemulsions at 293 K**

	$\tau_1$ (ns)	$\tau_2$ (ns)	$\tau_3$ (ns)	$A_1$ (%)	$A_2$ (%)	$A_3$ (%)	$r_{01}$	$r_{02}$	$\theta_1$ (ns)	$\theta_2$ (ns)
$S_{414}^a$	8.18	0.51		59	41		0			
$S_{406}^a$	7.81	0.45		52	48		-0.036			
$S_{490}^a$	3.69	0.82	0.11	2	2	96	0.026	0.084	>20 <sup>c</sup>	0.6
$S_{424}^b$	2.83	1.59	0.07	<1	<1	99	0.024	0.055	>20 <sup>c</sup>	0.5

<sup>a</sup> Emission at 660 nm. <sup>b</sup> Emission at 606 nm. <sup>c</sup> Much longer than our experimental temporal window.

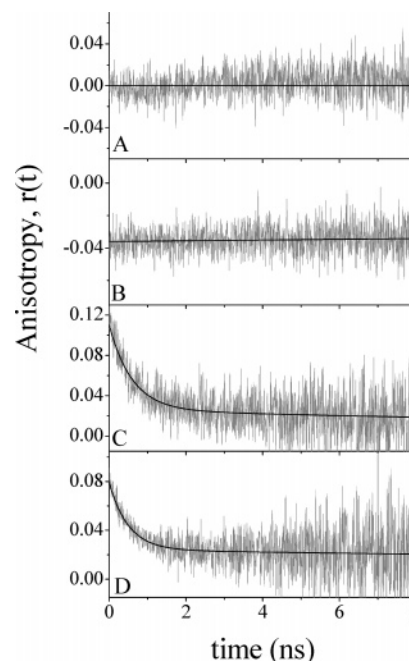
**Figure 8.** Time-resolved fluorescence decays for the  $S_{406}$  (A) and  $S_{424}$  (B) species (the solid lines represent the best-fit results). The weighted residuals indicate the goodness of the fit procedure.**Figure 9.** Time-resolved fluorescence decays for the  $S_{414}$  (A) and  $S_{490}$  (B) species (the solid lines represent the best-fit results). The weighted residuals indicate the goodness of the fit procedure.

Indeed, in aqueous solution, a typical porphyrin molecule shows a rotational correlation time ( $\tau_R$ ) of about 0.5 ns,<sup>64</sup> which is measurable with our instrumental apparatus.

On the contrary, in the case of  $S_{406}$ , the fluorescence becomes polarized with a negative  $r_0$  value of about -0.036 and a very long rotational correlation time, much longer than our experimental temporal window ( $\sim 10$  ns). Very different is the fluorescence anisotropy behavior of the species  $S_{490}$  and  $S_{424}$ . In these cases (see Table 2), the anisotropy decay is biexponential with a short rotational correlation time of about 0.5 ns and a very long one greater than 20 ns.

## Discussion

In aqueous bulk neutral solution (pH > 6), the porphyrin TPPS<sub>4</sub> is present as the unprotonated free base, and the UV-vis spectra are dominated by the intense B-band at 414 nm and by a series of four weaker Q-bands at 515, 551, 580, and 633 nm.<sup>64</sup> In a microemulsion environment, the biexponential fluorescence decay of the porphyrin in the case of the  $S_{414}$

**Figure 10.** Time-resolved anisotropy ( $r(t)$ ) of the various TPPS<sub>4</sub> species:  $S_{414}$  (A),  $S_{406}$  (B),  $S_{490}$  (C) and  $S_{424}$  (D).

sample is rather unusual. Indeed, the Soret band at 414 nm suggests that the chromophore is surely present as a tetra-anionic monomer dissolved in the water pool of the microemulsion, and consequently, its fluorescence decay should be monoexponential with a lifetime of 9.26 ns.<sup>64</sup> On the other hand, exciting at 570 nm and revealing the emission at 660 nm, this sample exhibits a completely depolarized fluorescence because of the fundamental anisotropy value ( $r_0$ ) equal to zero. In our experimental conditions, this value has been determined for a monomeric free base TPPS<sub>4</sub> aqueous solution.<sup>65</sup> To explain the apparently atypical behavior of the fluorescence decay of the porphyrin, we have to take into account that, in our sample, the chromophore (whose diameter is about 20 Å) is confined into a microemulsion that has a diameter of about 130 Å ( $w_0 = 32$ ). During the lifetime of its excited state ( $\sim 10$  ns), the TPPS<sub>4</sub> molecule exhibits a root-mean-square displacement of about 30–35 Å in water solution.<sup>66</sup> Consequently, the observed biexponential emission decay of TPPS<sub>4</sub> in the water pool can be ascribed to an inhomogeneous diffusional fluorescence quenching because of the probable collisions with the wall of the microemulsion: (i) the long-living emitting species ( $\sim 8$  ns) corresponds to molecules that are localized in the inner part of the water pool (the distance from the wall is greater than 30–35 Å, hence, the collision probability is very low and their emission is less quenched); (ii) the short-living species ( $\sim 0.5$  ns) are molecules close to the wall of the microemulsion (the distance is less than 30–35 Å), and consequently, their fluorescence emission is strongly quenched because of the high probability of collision with the internal wall.

In bulk neutral solutions, dimerization is achieved by adding specific reagents, such as crown ethers and alkali metal ions.<sup>12</sup>

This phenomenon is accompanied in the UV–vis spectra by hypochromicity and broadening of the B-band, together with a bathochromic shift of the Q-bands. As far as the S<sub>406</sub> sample is concerned, the corresponding Soret absorption feature (at 406 nm) can be deconvoluted into two bands, centered at 414 and 400 nm (data not shown); this latter component can be attributed to a H-dimer of the tetra-anionic TPPS<sub>4</sub>.<sup>33</sup> Consequently, the samples containing S<sub>406</sub>, obtained by changing the microemulsions size and/or increasing the porphyrin concentration, lead to a mixture of tetra-anionic porphyrin both as a monomer and a H-dimer. Because this latter evidences a fluorescence lifetime of about 8 ns,<sup>64</sup> the emission decay of the S<sub>406</sub> sample appears very similar to that of the S<sub>414</sub> one. On the contrary, the results of fluorescence anisotropy measurements appear to be very different because, in the case of S<sub>406</sub>, the emission becomes polarized with a negative  $r_0$  value of  $-0.036$  and a very long rotational correlation time. Because, under the same experimental conditions, the tetra-anionic monomeric TPPS<sub>4</sub> does not contribute to the polarization of the fluorescence emission, the measured anisotropy can be only ascribed to the H-dimer of the porphyrin. Moreover, the very long rotational correlation time clearly indicates that the TPPS<sub>4</sub> H-dimer is not free to rotate, probably because of its strong interaction with the internal wall of the microemulsion. Its fluorescence emission, therefore, is only depolarized by the overall rotational motion of the microemulsion, which, in the present case, has an hydrodynamic radius of about 60–70 Å.<sup>42</sup>

In the case of the S<sub>490</sub> sample, the very short fluorescent component ( $\tau = 0.11$  ns), which is the major one (relative amplitude of 96%), can be safely assigned to the J-aggregate form of the protonated diacid TPPS<sub>4</sub>.<sup>33</sup> The nature of this species is also confirmed by the narrow and red-shifted absorption peak at 490 nm and the presence of very intense peaks in the corresponding resonance light scattering spectra.<sup>19,42,53</sup> The other long-living emitting species ( $\tau = 3.69$  ns) detected in these samples can be attributed to the monomeric form of the diacid TPPS<sub>4</sub> (in good agreement with the lifetime value of 3.87 ns reported in the literature),<sup>64</sup> whereas the intermediate-living species could be some kind of oligomeric aggregate. This picture is consistent with the fluorescence anisotropy measurements which reveal the presence of two rotational correlation times: a short value (0.6 ns) due to both monomeric and oligomeric form of the porphyrin, and a longer one ( $>20$  ns), which can be ascribed to the J-aggregate. Because this latter value is much greater than that reported by Maiti et al. (10 ns),<sup>64</sup> we can suppose that, in our case, J-aggregates are strongly interacting with the internal wall of the microemulsions.

Finally, the case of the S<sub>424</sub> species appears controversial. This species is generally formed with a slow kinetic process starting from samples containing S<sub>414</sub> and S<sub>406</sub>. Its Soret absorption band is centered at 424 nm, and the presence of two Q-bands suggests the protonation of the central nitrogen core (i.e., a diacid porphyrin). Therefore, the B-band is blue-shifted with respect to that of the diacid TPPS<sub>4</sub> centered at 434 nm.<sup>33</sup> Time-resolved fluorescence and fluorescence anisotropy data seem very similar to those obtained in the case of S<sub>490</sub>. Anyway, in the case of S<sub>424</sub>, fluorescence emission spectra show a band at 606 nm, which is consistently blue-shifted with respect to the emission spectra of the other forms of TPPS<sub>4</sub>. Because the blue-shift of the B-band can be the result of an H-type aggregation process, the optical absorption spectra seem to suggest that, in the S<sub>424</sub> species, the porphyrin molecules are prevalently present as H-dimer and/or H-aggregate of the diacid form. The time-resolved fluorescence experiments reveal the

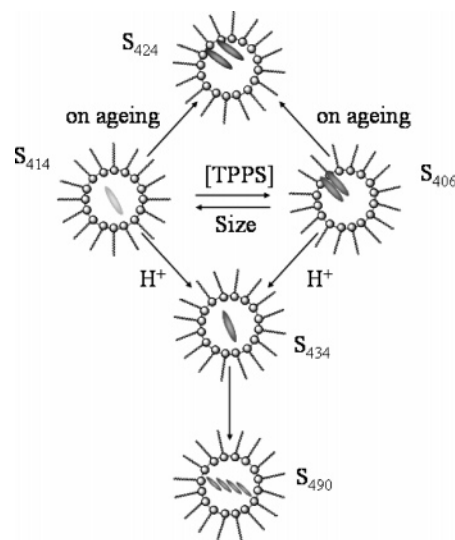


**Figure 11.** Pictorial sketch for the proposed various TPPS<sub>4</sub> species and their interconversion inside AOT/water/decane microemulsions as a function of water pool size, pH, porphyrin concentration, and aging.

occurrence of a predominant short-living emitting species (relative amplitude of 99%) with a lifetime value of 0.07 ns, which is much shorter than the diacid monomer (3.87 ns). On the other hand, the fluorescence lifetime of an H-dimer is expected to be similar to or greater than that of the monomer, whereas a value significantly smaller than that of the monomer is associated with the J-dimer formation.<sup>64,67</sup> This discrepancy, together with the observed anomalous kinetic behavior of this species, calls for further investigations.

**Concluding Remarks.** All our experimental findings point to the presence of different species confined in these microemulsions as function of the various investigated parameters. Figure 11 reports a pictorial sketch of the proposed model for their interconversion.

In the inner water compartment of these microemulsions, under neutral pH conditions, the porphyrin is present as the free base monomer (S<sub>414</sub>) in the case of high  $w_0$  values, i.e., when the inner pool is large enough to prevent an entanglement process with the surfactant molecules. These species are also stabilized when the porphyrin concentration is low. An H-dimer of the unprotonated porphyrin (S<sub>406</sub>) is formed on increasing the TPPS<sub>4</sub> concentration and reducing the size of the water pool. This species is mainly blocked close to the palisade, and consequently, its tumbling motion is related to the whole microemulsion. Both the free monomeric species and this latter dimer evidence a slow conversion to a dimeric form of the diacid porphyrin, which has been postulated to have a H-type geometrical arrangement (S<sub>424</sub>). This kinetic process can be probably ascribed to protonation of the inner nitrogen core because of a higher hydrogen ion concentration in close proximity of the negatively charged sulfonate headgroups of AOT molecules.<sup>47</sup> On decreasing the pH, except for S<sub>424</sub>, all the various species rapidly convert to the monomeric diacid porphyrin (S<sub>434</sub>), which eventually leads to the formation of J-aggregates (S<sub>490</sub>). The knowledge of the thermodynamic stability and interconversion pattern for this confined system allows for a detailed investigation of the spectroscopic and photophysical properties of the various species. Furthermore, a fine-tuning of the optical properties of such aggregates in terms of size and structural arrangement, or the possibility of obtaining hetero-aggregated species introducing different porphyrins or their metalloderivatives, opens the way to their potential applications in nanocatalysis or optoelectronics.



**Acknowledgment.** We thank MIUR (PRIN-COFIN 2004) and CNR for financial support.

**Supporting Information Available:** Graphs showing time evolution UV–vis spectra for different  $w_0$  values (6–65) of samples of TPPS<sub>4</sub> in AOT/water/decane microemulsions and samples of TPPS<sub>4</sub> in AOT/water/decane microemulsions at different increasing porphyrin concentrations; UV–vis spectra of samples of TPPS<sub>4</sub> J-aggregates in AOT/water/decane microemulsions at different increasing porphyrin concentrations. This material is available free of charge via the Internet at <http://pubs.acs.org>.

**Note Added after ASAP Publication.** There was an error in that the Supporting Information paragraph was omitted in the version published ASAP May 26, 2005; the corrected version was published ASAP June 6, 2005.

## References and Notes

- (1) White, W. I. In *The Porphyrins*; Dolphin, D., Ed.; Academic Press: New York, 1978; Vol. 5, p 303.
- (2) McRae, E. G.; Kasha, M. *J. Chem. Phys.* **1958**, *28*, 721.
- (3) McRae, E. G.; Kasha, M. In *Physical Processes in Radiation Biology*; Augenstein, L.; Mason, R.; Rosenberg, B., Eds.; Academic Press: New York, 1964; p 23.
- (4) Schwab, A. D.; Smith, D. E.; Rich, C. S.; Young, E. R.; Smith, W. F.; de Paula, J. C. *J. Phys. Chem. B* **2003**, *107*, 11339.
- (5) Kobayashi, T. *Supramol. Sci.* **1998**, *5*, 343.
- (6) Kano, H.; Saito, T.; Kobayashi, T. *J. Phys. Chem. B* **2001**, *105*, 413.
- (7) Kano, H.; Saito, T.; Kobayashi, T. *J. Phys. Chem. A* **2002**, *106*, 3445.
- (8) Kano, H.; Kobayashi, T. *J. Chem. Phys.* **2002**, *116*, 184.
- (9) Collini, E.; Ferrante, C.; Bozio, R. *J. Phys. Chem. B* **2005**, *109*, 2.
- (10) Schwab, A. D.; Smith, D. E.; Bond-Watts, B.; Johnston, D. E.; Hone, J.; Johnson, A. T.; de Paula, J. C.; Smith, W. F. *Nano Lett.* **2004**, *4*, 1261.
- (11) Kalyanasundaram, K. *Photochemistry of Polypyridine and Porphyrin Complexes*; Academic Press: London, 1992.
- (12) Chandrashekar, T. K.; Van Willigen, H.; Ebersole, M. H. *J. Phys. Chem.* **1984**, *88*, 4326.
- (13) Ohno, O.; Kaizu, Y.; Kobayashi, H. *J. Chem. Phys.* **1993**, *99*, 4128.
- (14) Pasternack, R. F.; Schaefer, K. F.; Hambright, P. *Inorg. Chem.* **1994**, *33*, 2062.
- (15) Ribo, J. M.; Crusats, J.; Farrera, J. A.; Valero, M. L. *J. Chem. Soc., Chem. Commun.* **1994**, 681.
- (16) Akins, D. L.; Ozcelik, S.; Zhu, H. R.; Guo, C. *J. Phys. Chem.* **1996**, *100*, 14390.
- (17) Akins, D. L.; Zhu, H. R.; Guo, C. *J. Phys. Chem.* **1996**, *100*, 5420.
- (18) Guo, C.; Ren, B.; Akins, D. L. *J. Phys. Chem. B* **1998**, *102*, 8751.
- (19) Collings, P. J.; Gibbs, E. J.; Starr, T. E.; Vafek, O.; Yee, C.; Pomerance, L. A.; Pasternack, R. F. *J. Phys. Chem. B* **1999**, *103*, 8474.
- (20) Rubires, R.; Crusats, J.; El-Hachemi, Z.; Jaramillo, T.; Lopez, M.; Valls, E.; Farrera, J. A.; Ribo, J. M. *New J. Chem.* **1999**, *23*, 189.
- (21) Micali, N.; Romeo, A.; Lauceri, R.; Purrello, R.; Mallamace, F.; Sclaro, L. M. *J. Phys. Chem. B* **2000**, *104*, 9416.
- (22) Micali, N.; Mallamace, F.; Romeo, A.; Purrello, R.; Sclaro, L. M. *J. Phys. Chem. B* **2000**, *104*, 5897.
- (23) Ren, B.; Tian, Z. Q.; Guo, C.; Akins, D. L. *Chem. Phys. Lett.* **2000**, *328*, 17.
- (24) Ribo, J. M.; Crusats, J.; Sagues, F.; Claret, J.; Rubires, R. *Science* **2001**, *292*, 2063.
- (25) Rubires, R.; Muller, C.; Campos, L.; El-Hachemi, Z.; Pakhomov, G. L.; Ribo, J. M. *J. Porphyrins Phthalocyanines* **2002**, *6*, 107.
- (26) Castriciano, M. A.; Romeo, A.; Villari, V.; Micali, N.; Sclaro, L. M. *J. Phys. Chem. B* **2003**, *107*, 8765.
- (27) Gandini, S. C. M.; Gelamo, E. L.; Itri, R.; Tabak, M. *Biophys. J.* **2003**, *85*, 1259.
- (28) Koti, A. S. R.; Periasamy, N. *Chem. Mater.* **2003**, *15*, 369.
- (29) Rotomskis, R.; Augulis, R.; Snitka, V.; Valiokas, R.; Liedberg, B. *J. Phys. Chem. B* **2004**, *108*, 2833.
- (30) Knapp, E. W. *Chem. Phys.* **1984**, *85*, 73.
- (31) Gandini, S. C. M.; Yushmanov, V. E.; Borissevitch, I. E.; Tabak, M. *Langmuir* **1999**, *15*, 6233.
- (32) Maiti, N. C.; Mazumdar, S.; Periasamy, N. *J. Porphyrins Phthalocyanines* **1998**, *2*, 369.
- (33) Maiti, N. C.; Mazumdar, S.; Periasamy, N. *J. Phys. Chem. B* **1998**, *102*, 1528.
- (34) Jiang, S. G.; Liu, M. H. *J. Phys. Chem. B* **2004**, *108*, 2880.
- (35) Zhang, L.; Yuan, J.; Liu, M. H. *J. Phys. Chem. B* **2003**, *107*, 12768.
- (36) Xu, W.; Guo, H. Q.; Akins, D. L. *J. Phys. Chem. B* **2001**, *105*, 1543.
- (37) Paulo, P. M. R.; Gronheid, R.; De Schryver, F. C.; Costa, S. M. B. *Macromolecules* **2003**, *36*, 9135.
- (38) Paulo, P. M. R.; Costa, S. M. B. *Photochem. Photobiol.* **2003**, *2*, 597.
- (39) Purrello, R.; Sclaro, L. M.; Bellacchio, E.; Gurrieri, S.; Romeo, A. *Inorg. Chem.* **1998**, *37*, 3647.
- (40) Castriciano, M. A.; Romeo, A.; Sclaro, L. M. *J. Porphyrins Phthalocyanines* **2002**, *6*, 431.
- (41) Purrello, R.; Bellacchio, E.; Gurrieri, S.; Lauceri, R.; Raudino, A.; Sclaro, L. M.; Santoro, A. M. *J. Phys. Chem. B* **1998**, *102*, 8852.
- (42) Castriciano, M. A.; Romeo, A.; Villari, V.; Micali, N.; Sclaro, L. M. *J. Phys. Chem. B* **2004**, *108*, 9054.
- (43) Amico, P.; Dangelo, M.; Onori, G.; Santucci, A. *Nuovo Cimento Soc. Ital. Fis. D* **1995**, *17*, 1053.
- (44) Christopher, D. J.; Yarwood, J.; Belton, P. S.; Hills, B. P. *J. Colloid Interface Sci.* **1992**, *152*, 465.
- (45) Onori, G.; Santucci, A. *J. Phys. Chem.* **1993**, *97*, 5430.
- (46) Hauser, H.; Haering, G.; Pande, A.; Luisi, P. L. *J. Phys. Chem.* **1989**, *93*, 7869.
- (47) El Seoud, O. A. Acidities and Basicities in Reversed Micellar Systems. In *Reverse Micelles: Biological and Technological Relevance of Amphiphilic Structures in Apolar Media*; Luisi, P. L.; Straub, B. E., Eds.; Plenum Press: New York, 1984; p 81.
- (48) Aoudia, M.; Rodgers, M. A. J. *J. Phys. Chem. B* **2003**, *107*, 6194.
- (49) Togashi, D. M.; Costa, S. M. B. *Phys. Chem. Chem. Phys.* **2000**, *2*, 5437.
- (50) Togashi, D. M.; Costa, S. M. B. *Phys. Chem. Chem. Phys.* **2002**, *4*, 1141.
- (51) Togashi, D. M.; Costa, S. M. B.; Sobral, A.; Gonsalves, A. *J. Phys. Chem. B* **2004**, *108*, 11344.
- (52) Koti, A. S. R.; Taneja, J.; Periasamy, N. *Chem. Phys. Lett.* **2003**, *375*, 171.
- (53) Pasternack, R. F.; Collings, P. J. *Science* **1995**, *269*, 935.
- (54) Knyukshto, V. N.; Solov'yov, K. N.; Egorova, G. D. *Biospectroscopy* **1998**, *4*, 121.
- (55) Berne, B. J.; Pecora, R. *Dynamic Light Scattering*; Wiley-Interscience: New York, 1976.
- (56) Corti, M.; Degiorgio, V. *Phys. Rev. Lett.* **1980**, *45*, 1045.
- (57) Corti, M.; Degiorgio, V. *J. Phys. Chem.* **1981**, *85*, 711.
- (58) Corti, M. In *Physics of Amphiphiles: Micelles, Vesicles and Microemulsions*; Degiorgio, V.; Corti, M., Eds.; North-Holland: Amsterdam, 1985.
- (59) Corti, M.; Degiorgio, V. *Phys. Rev. Lett.* **1985**, *55*, 2005.
- (60) O'Connor, D. V.; Phillips, D. *Time-Correlated Single Photon Counting*; Academic Press: New York, 1984.
- (61) Angelini, N.; Micali, N.; Villari, V.; Mineo, P.; Vitalini, D.; Scamporrino, E. *Phys. Rev. E* **2005**, *71*, 21915.
- (62) Marquardt, D. W. *J. Soc. Ind. Appl. Math.* **1969**, *11*, 431.
- (63) Lakowicz, J. R. *Principles of Fluorescence Spectroscopy*; Kluwer Academic/Plenum Publishers: New York, 1999.
- (64) Maiti, N. C.; Ravikanth, M.; Mazumdar, S.; Periasamy, N. *J. Phys. Chem.* **1995**, *99*, 17192.
- (65) Mazzaglia, A.; Angelini, N.; Lombardo, D.; Micali, N.; Patanè, S.; Villari, V.; Monsu' Sclaro, L. *J. Phys. Chem. B* **2005**, *109*, 7258.
- (66) Note: root-mean-square displacement ( $l$ ) is defined on the basis of the following equation:  $l = \sqrt{6D\tau} = \sqrt{(k_B T / \pi R \eta) \tau}$  where:  $D$  is the diffusion coefficient,  $\tau$  is the fluorescence lifetime (10 ns),  $k_B$  is the Boltzmann constant,  $T$  is the absolute temperature (300 K),  $R$  is the porphyrin radius (10 Å), and  $\eta$  is the water viscosity.
- (67) Barber, D. C.; Freitagbeeston, R. A.; Whitten, D. G. *J. Phys. Chem.* **1991**, *95*, 4074.